Two types of mirror mode waves in the Kronian magnetosheath

XinYa Duanmu[1,2], ZhongHua Yao[1,2*], Yong Wei[1,2], and ShengYi Ye[3]

[1]Key Laboratory of Earth and Planetary Physics, Institute of Geology and Geophysics, Chinese Academy of Sciences, Beijing 100029, China;

[2]College of Earth and Planetary Sciences, University of Chinese Academy of Sciences, Beijing 100049, China;

[3]Department of Earth and Space Sciences, Southern University of Science and Technology, Shenzhen Guangdong 518055, China

Key Points:
- Two types of mirror mode waves, peaks and dips, can be observed in the Kronian magnetosheath and show different characteristics.
- The frequency and amplitude of mirror mode waves may evolve from the bow shock to the magnetopause.
- Mirror mode waves and electromagnetic ion cyclotron waves can coexist in the Kronian magnetosheath.

Abstract: A mirror mode wave is a fundamental magnetic structure in the planetary space environment that is persistently compressed by solar wind, especially in the magnetosheath. Mirror modes have been widely identified in the magnetosheaths of the Earth and other planets in the solar system, yet the understanding of mirror mode waves on extraterrestrial planets is not as comprehensive as that on the Earth. Using magnetic field data collected by the Cassini spacecraft, we found peak and dip types according to the magnetic morphology (i.e., structures with higher or lower magnetic strengths than the background field). Moreover, mirror mode waves and electromagnetic ion cyclotron waves were found one after the other, implying that the two wave modes may evolve into one another in the Kronian magnetosheath. The results indicate that many fundamental plasma processes associated with the mirror mode structure exist in the Kronian magnetosheath. The energy conversion in Saturn's magnetosheath may provide key insights that will aid in understanding giant planetary magnetospheric processes.

1. Introduction

The mirror mode wave (MMW) is a nonpropagating wave in the rest frame of the plasma and is a typical magnetic bottle structure in space. It traps high-density plasma in the pocket and drifts together with the surrounding plasma. Thus, in observational data, an MMW often appears as a sudden drop or peak in magnetic field strength and is inversely correlated with changes in plasma density (Tsurutani et al., 2011).

Mirror mode structures are commonly observed in solar system plasma environments and widely exist in planetary magnetosheaths (e.g., Tsurutani et al., 1982; Violante et al., 1995; Cattaneo et al., 1998; Volwerk et al., 2008a, b, 2014; Zhang TL et al., 2009; Soucek et al., 2015), planetary magnetospheres (Russell et al., 1998, 2006), cometary magnetic environments (Russell et al., 1987; Mazelle et al., 1991; Glassmeier et al., 1993; Volwerk et al., 2016), and the solar wind (Kaufmann et al., 1970; Winterhalter et al., 1995). In competition with Alfvén ion cyclotron waves, with which they are cogenerated in the same plasma environment (Shoji et al., 2009), MMWs are compressional waves with a low

frequency in the observations and often with large amplitudes under high beta plasma conditions (i.e., the ratio of plasma to magnetic pressure) and ion temperature anisotropy (Hasegawa, 1969).

The MMW in the magnetosheath features mainly quasi-periodic large-scale fluctuations, showing magnetic peak and dip structures that are classified based on the amplitude of perturbation to the background magnetic field. For example, Joy et al. (2006) divided the MMW in Jupiter's magnetosheath into three categories (i.e., peaks, dips, and others). Génot et al. (2009) proposed the skewness method to classify the types of MMWs. They suggested that the peak and dip types of MMWs may evolve into each other in the terrestrial magnetosheath. To understand the evolution of MMWs, Cattaneo et al. (1998) proposed a qualitative empirical model for their evolution in the Kronian magnetosheath, which was later confirmed and extended by Joy et al. (2006) in the Jovian system. These studies showed that MMWs are mainly generated near the bow shock and that they develop by propagating on the way to the magnetopause. During this process, the wave amplitude increases, and nonlinear saturation may occur. Magnetic peaks appear more frequently near the middle magnetosheath, and magnetic dips often appear near the magnetopause, where the plasma environment becomes mirror-stabilized and the mirror structure begins to collapse and decay. In contrast, Tátrallyay and Erdős (2005) suggested that the mirror mode may not always orig-

inate near the bow shock, based on the measured MMW growth rate being an order of magnitude lower than expected. Increased anisotropy can be a significant source of mirror instability.

Mirror modes were reported at Jupiter and Saturn by Pioneer 11 (Tsurutani et al., 1982) and in the subsolar magnetosheath of Saturn by Voyagers 1 and 2 (Violante et al., 1995). Cattaneo et al. (1998) studied the evolution of Saturn's subsolar magnetosheath mirror mode structure by using the plasma and magnetic field data of Voyagers 1 and 2. Later, research on the mirror mode in Saturn mainly focused on the magnetosphere rather than the magnetosheath. The Cassini data set provides a comprehensive observation of Saturn's magnetosheath and shows that three aspects of Saturn's magnetosheath plasma properties are quite different from those of the terrestrial magnetosheath: their higher values (the ratio of the upstream solar wind speed to the Alfvénic wave speed) in the upstream solar wind (Sulaiman et al., 2015, 2016), higher magnetosheath values (~10–100; Thomsen et al., 2018), and predominant quasi-perpendicular shock geometries (Achilleos et al., 2006; Sulaiman et al., 2016).

In this study, we surveyed the Cassini data set and identified two types of mirror mode structures. In addition to the two types of mirror modes, we found that the mirror mode wave and the electromagnetic ion cyclotron (EMIC) wave may convert to each other. The potential importance of these results and investigations continuing into the future are also discussed.

2. Observations

2.1 Identification and Classification of MMWs

The identification of a mirror mode is based on the change in plasma density as opposed to the magnetic field strength. The ion data of Cassini were often insufficient because of the limited field of view of the instrument; nevertheless, magnetic field data can be useful for identifying mirror mode events. The magnetic data were analyzed by using the method described by Lucek et al. (1999). Mirror modes in magnetic field data can be characterized by large-amplitude perturbations in the field strength that are generally linearly polarized and aligned with the background field in a maximum variance direction (Lucek et al., 1999; Price et al., 1986; Génot et al., 2001). Cattaneo et al. (1998) studied mirror modes in Saturn's magnetosheath by using data provided by the magnetic field and plasma experiments on Voyagers 1 and 2. They found that the angle between the maximum variance and the background magnetic field of the mirror mode is generally less than 30°, whereas the angle between the minimum variance and the background magnetic field is from 60° to 80°, with $\Delta B/B$ ranging from 0.1 to 0.3 or higher. On the basis of these findings, we selected MMWs according to two criteria: (1) $\theta_{B,\max} < 80°$ and $\theta_{B,\min} > 80°$, and (2) $\delta B_{//}/B_0 > 0.2$.

We used these criteria to identify mirror structures in the field data. First, a 20'-wide sliding window minimum variance analysis was performed, with a shift of 1'. To identify MMWs, we determined the angles between the maximum ($\theta_{B,\max}$) and minimum ($\theta_{B,\min}$) variance directions and the background magnetic field for each point in the sliding window. For each point, we then determined the strength (δB) of the waves in the data as the maximum differ-

ence from the mean field.

The overview of a magnetosheath crossing shown in Figure 1 presents clear MMW signatures. Shown are the (a) total magnetic strength, (b) three components of the magnetic fields in Kronian range-θ-ϕ (KRTP) coordinates (i.e., magnetic field vector components form the standard right-handed spherical triad (R, θ, ϕ) for a planet-centered system, where R is radial from Saturn to the center of the spacecraft, ϕ indicates the azimuthal component that is parallel to the Kronographic equator, and θ completes the right-handed set), and (c−e) the magnetic field components in field-aligned coordinates. The mean magnetic field averaged over 20' is taken as the $+z$ direction, and the two vectors perpendicular to the mean field direction complete the right-handed coordinate system. In Figure 1f, $\theta_{B,\max}$ and $\theta_{B,\min}$ are the angles between the direction of the maximum or minimum variance and the direction of the background magnetic field. Figure 1g shows the proportional strengths of the parallel component $\delta B_{//}/|B|$ and the two perpendicular components $\delta B_{\perp 1}/|B|$ and $\delta B_{\perp 2}/|B|$ of fluctuations.

The magnetosheath crossing event was detected between the bow shock encounter at 20:37 coordinated universal time (UTC) on July 29, 2005, and the magnetopause encounter at 12:20 UTC on July 30, 2005. The MMWs are highlighted by the pink shadow. The total magnetic field shows large amplitude fluctuations during this period. The compression component $B_{//}$ plays a major role, with $\delta B_{/}/B_0 > 0.2$, $\delta B_{\perp 1}/|B|$ and $\delta B_{\perp 2}/|B|$ almost < 0.2, and the maximum variance direction below 30°. In this period, a limited number of subperiods do not satisfy the selection criteria. These subperiods satisfy the selection criteria $\theta_{B,\max} < 30°$ and $\delta B_{//}/|B| > 0.2$, whereas $\theta_{B,\min}$ is between 60° and 80°. They were not intentionally marked in this event because they actually satisfy the MMW characteristics of Cattaneo et al. (1998). The strict constraint of $\theta_{B,\min} > 80°$ is expected to be nearly perpendicular for MMWs, allowing better data selection to complete subsequent statistical research.

On the basis of the magnetic morphologies, MMWs can be classified as peaks, dips, and quasi-periodic (others) by the skewness method (Génot et al., 2009). Skewness is a statistical parameter that describes the symmetry of data distribution. Positive skewness suggests that the majority of data points are located below the mean value, whereas negative skewness indicates the opposite. A skewness value of zero implies that the data points are perfectly symmetrically distributed. When examining the magnetic field amplitude, positive skewness represents a peak-like structure, whereas negative skewness reflects a dip-like structure. In the calculation of skewness in this study, the background magnetic field was average, with a 20' window, and the skewness was calculated in a 15' window with a 1' sliding step. The 15' window selected here was estimated according to the observational features of the MMW, to ensure that at least two to three wave periods were included in each calculation. The results in Figure 2 clearly demonstrate that peak-type MMWs have positive skewness and dip-type MMWs have negative skewness. From our experience, >0.5 and <−0.5 would be good criteria for determining peak-type and dip-type MMWs. These criteria would be useful for future statistical investigations.
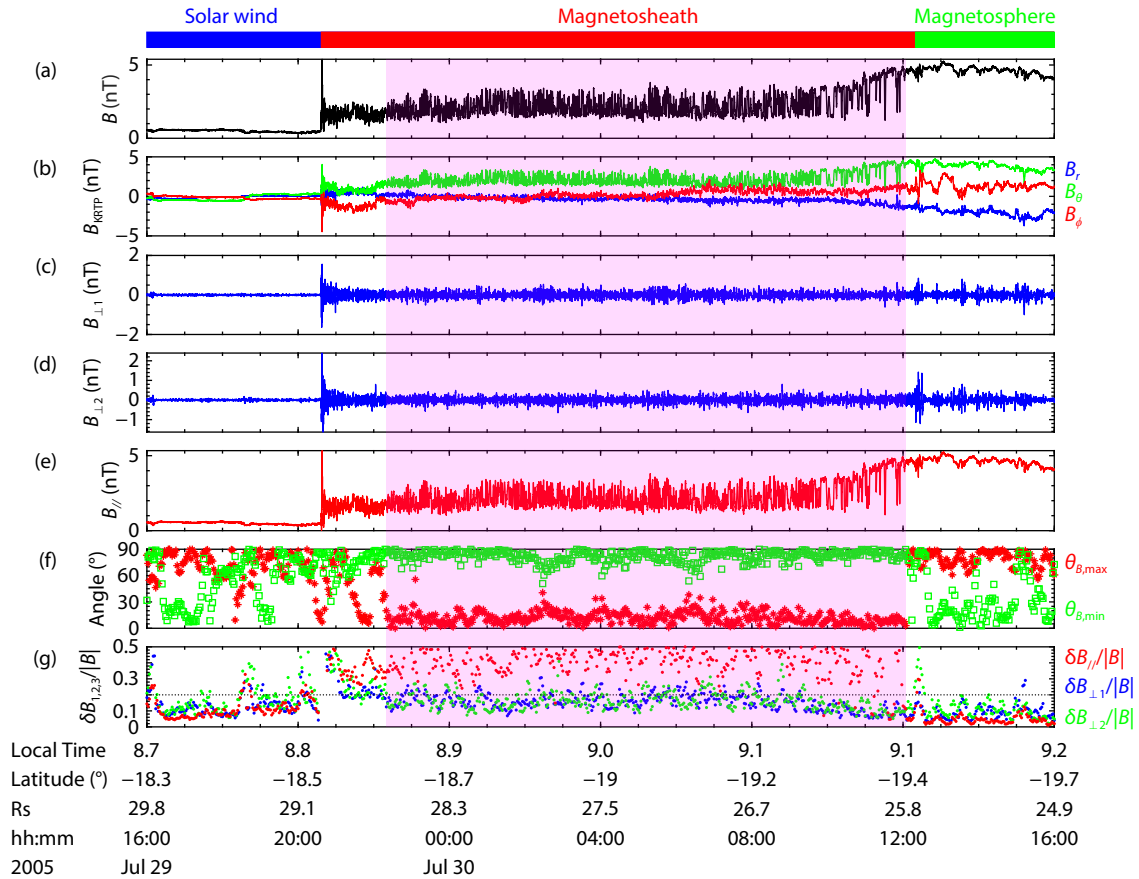
Figure 1. Example of mirror mode intervals identified on July 29–30, 2005. (a) The magnetic strength. (b) Three components of the magnetic field in Kronian range-θ-ϕ (KRTP) coordinates. (c–e) Magnetic field components in field-aligned coordinates. (f) Angle between the direction of the maximum or minimum variance and the direction of the background magnetic field $\theta_{B,max}$ (red asterisks) and $\theta_{B,min}$ (green squares). (g) Ratio of parallel and perpendicular components of the magnetic field to the total magnetic field $\delta B_{//}/|B|$ (red dots), $\delta B_{\perp 1}/|B|$ (blue dots), and $\delta B_{\perp 2}/|B|$ (green dots).
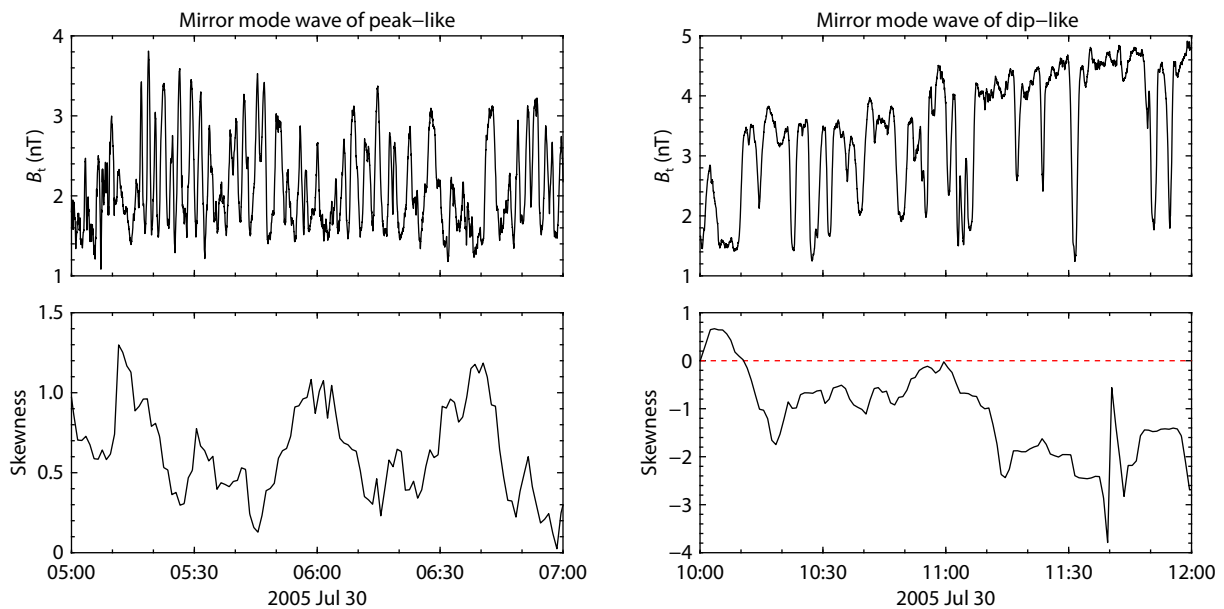

Figure 2. Two types of mirror mode waves (MMWs) from the subperiods in Figure 1. (Left panels) Peak-type MMW with large positive skewness. (Right panels) Dip-type MMW with large negative skewness.

Duanmu XY and Yao ZH et al.: Two types of mirror mode waves in the Kronian magnetosheath

2.2 Characteristics of the Two Types of MMWs

Figure 3 shows the variation characteristics of the skewness and amplitude of the MMWs. The red vertical line indicates the time (09:32:02 UTC) when the skewness changed from positive to negative, suggesting that the peak-type MMW may evolve to a dip-type MMW toward the magnetopause. Moreover, the frequency and wave amplitude may also evolve from the bow shock to the magnetopause. As shown in the third graph in Figure 3a, the wave amplitude increases from the bow shock to the magnetopause, which may correspond to temporal evolution during wave propagation. Power spectra of the field components (i.e., parallel and perpendicular) were calculated near the bow shock (Figure 3b), in the middle magnetosheath (Figure 3c), and near the magnetopause (Figure 3d). The parallel component was the dominant perturbation during the three selected periods, whereas the frequency was slightly smaller from the bow shock to the magnetopause, which may be associated with wave evolution on a greater spatial scale.

2.3 Example of the Coexistence of an MMW and an EMIC

Figure 4 shows another example of a MMW in the Kronian magnetosheath from 14:00 UTC on March 12, 2007, to 18:00 UTC on March 13, 2007. In this event, the EMIC wave is also detected,

which perhaps suggests wave mode conversion. Figure 4a shows the three magnetic components in the KRTP coordinate system. Figures 4b–d show the perpendicular and parallel magnetic components. In general, the magnetic perturbations were mostly parallel. Nevertheless, as highlighted by the pink shadow, there was a short period when the magnetic perturbation was mainly in a perpendicular direction. As shown by the power spectral density in Figure 4e, the wave frequency was generally well below the ion gyrofrequency, whereas in the pink shadow, the wave frequency was just below the ion gyrofrequency, which is a typical feature of an EMIC wave. Figures 4f–h show the degree of polarization (1 for a pure state wave and < 0.7 for noise), the wave normal angle (the angle between the ambient magnetic field averaged over 20′ and the wave normal vector), and the ellipticity ε, where ε is +1 for circular right-hand polarization, −1 for circular left-hand polarization, and 0 for linear polarization. The wave in the pink shadow was mainly left-handed and quasi-parallel to the magnetic field, providing further evidence this was an EMIC wave. This method can better identify an EMIC wave in combination with the transverse wave characteristics of the left-handed polarization of EMIC waves. Figures 4i and 4j further confirm that the perturbation was mainly perpendicular during the pink shadow but was mainly parallel during the rest time in the magnetosheath.
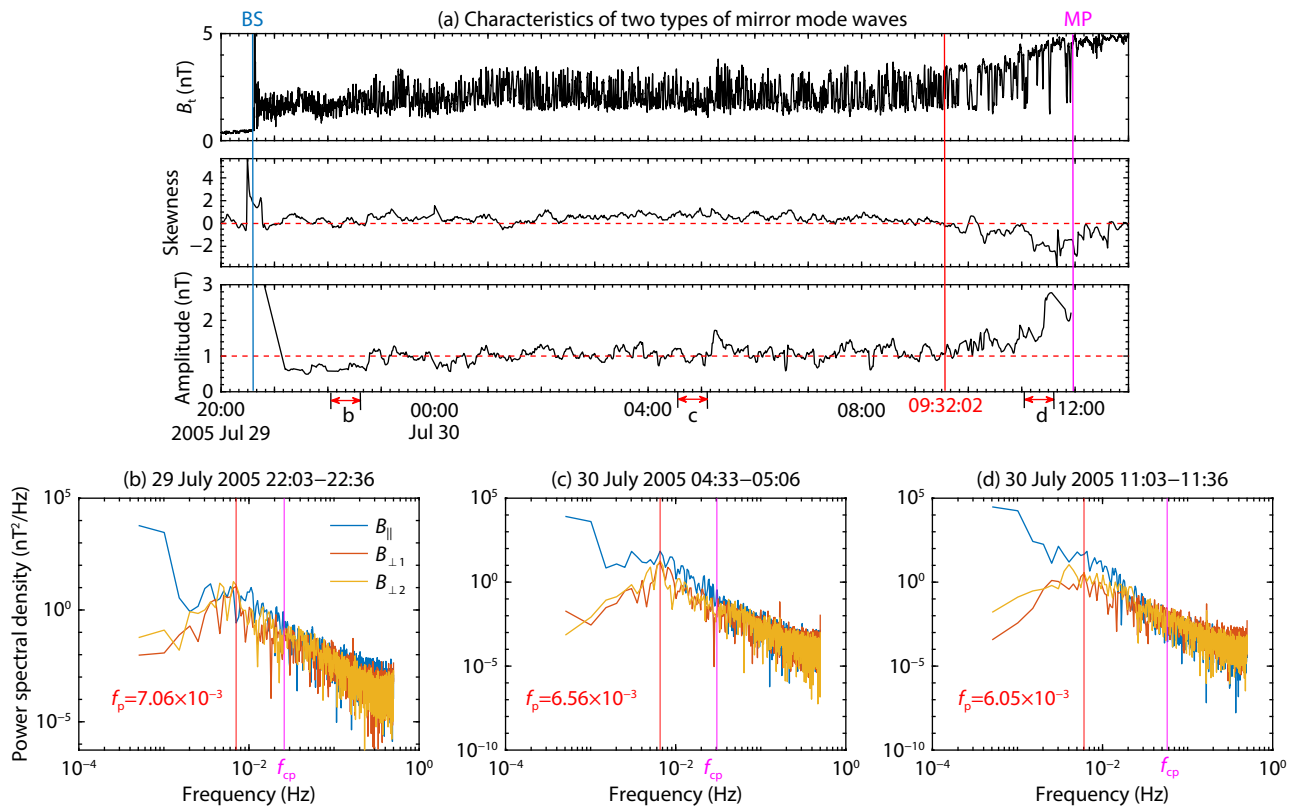

Figure 3. (a) The total strength, skewness, and amplitude of the magnetic fluctuations. The blue and pink vertical lines indicate the bow shock (BS) crossing time and the magnetopause (MP) crossing time. The red vertical line indicates the time (09:32:02 coordinated universal time (UTC)) when the skewness changed from positive to negative. (b–d) Power spectra of the field components parallel ($B_{//}$) and perpendicular ($B_{\perp 1}$ and $B_{\perp 2}$) to the average direction of B in the time intervals near the magnetopause (b), in the middle magnetosheath (c), and near the magnetopause (d). The pink vertical line in each plot indicates the proton gyrofrequency (f_{cp}), and the red vertical lines indicate the frequency with peak power spectral density (f_p).

Duanmu XY and Yao ZH et al.: Two types of mirror mode waves in the Kronian magnetosheath
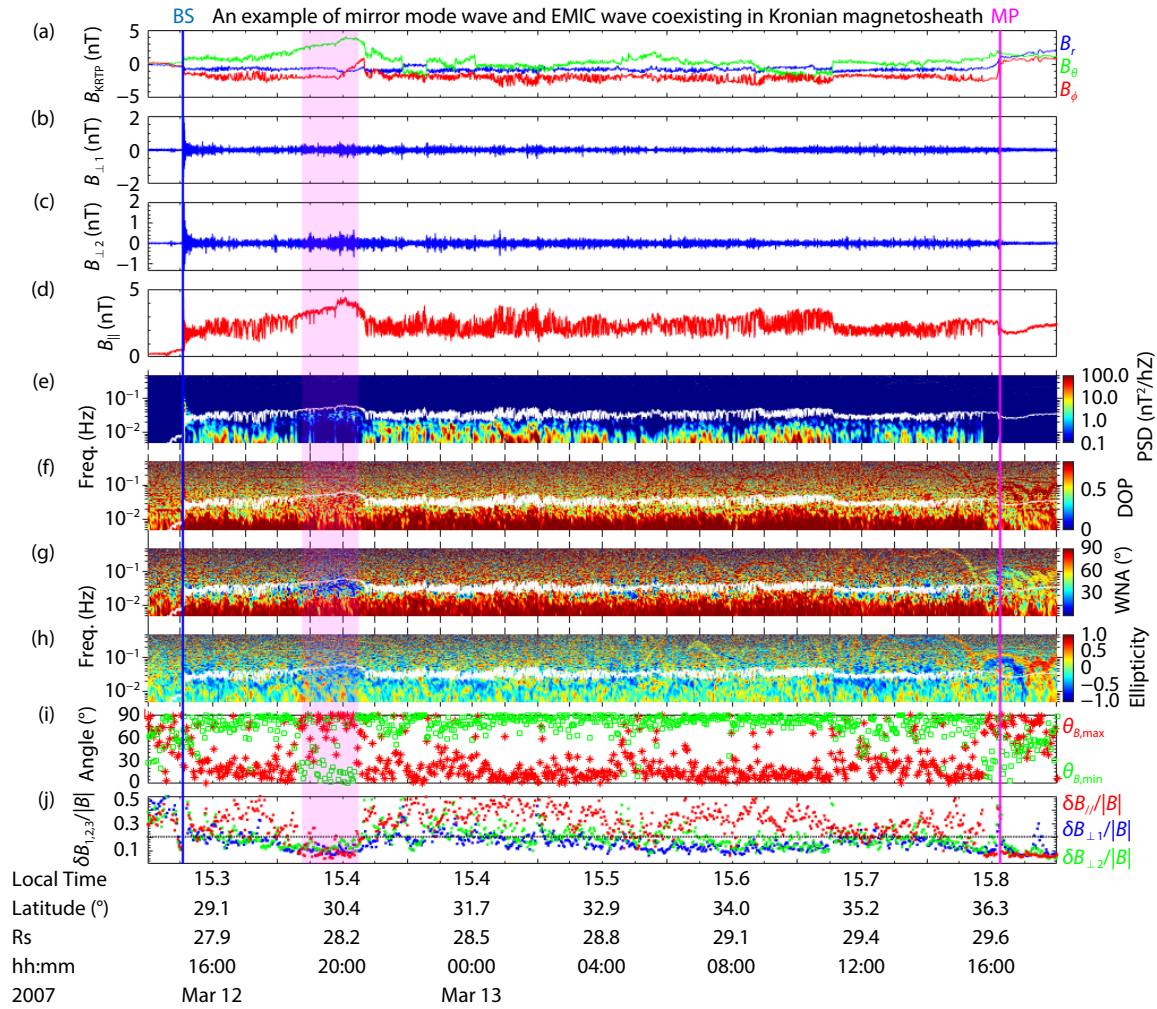
Figure 4. Overview of an event from 14:00 coordinated universal time (UTC) on March 12, 2007, to 18:00 UTC on March 13, 2007, showing both mirror mode wave (MMW) and electromagnetic ion cyclotron (EMIC) structures. (Top to bottom) (a) Three components of the 1-Hz magnetic field in Kronian range-θ-ϕ (KRTP) coordinates. (b–d) The magnetic field components in field-aligned coordinates. (e–h) Magnetic field power spectral density (PSD), degree of polarization (DOP), wave normal angle (WNA), and ellipticity. The white curves mark the local proton gyrofrequency, (i) the angle between the direction of the maximum and minimum variances and the background magnetic field $\theta_{B,max}$ (red asterisks) and $\theta_{B,min}$ (green squares), (j) the proportional strengths of the parallel components of the fluctuations $\delta B_{//}/|B|$ and the two perpendicular components $\delta B_{\perp1}/|B|$, $\delta B_{\perp2}/|B|$. The blue and purple lines indicate the bow shock (BS) crossing and the magnetopause (MP) crossing.

3. Discussion and Summary

Saturn's magnetosheath has high plasma beta (i.e., the ratio between plasma pressure and magnetic pressure), which is favorable for exciting MMW as well as EMIC fluctuations. In this study, we investigated two periods of Cassini observations in the Kronian magnetosheath. From the analysis of the two observations, we identified two types of MMWs (i.e., peak-type and dip-type) and suggest that the two types of MMWs may be converted during propagation. In general, the wave amplitude may increase during propagation from the bow shock to the magnetopause. Such a trend was also reported by Cattaneo et al. (1998) and Joy et al. (2006). Nevertheless, for a specific magnetosheath crossing, the amplitude evolution is not always clear. Sometimes the trend can even be opposite that of the statistical results.

Moreover, MMWs and EMIC waves may coexist in the magnetosheath, potentially suggesting that the two types of structures could be converted, which is similar in character to the terrestrial magnetosheath (Shoji et al., 2009). A possible reason for the coexistence of two wave transitions is the low plasma beta conditions. Although the magnetosheath of Saturn mostly exists under high beta plasma conditions, very few low beta plasma conditions can exist (Thomsen et al., 2018). When the magnetosheath is in a low beta condition with high temperature anisotropy (perpendicularly dominated), the ion cyclotron instability will be excited. The plasma beta and the perpendicular temperature anisotropy in different regions of the magnetosheath are different and can be time varying. This may lead to wave conversion and thus the coexistence of the two types of fluctuations. The mechanism in Saturn's magnetosheath will be investigated further.

Mirror mode waves are often generated near the bow shock, and then propagate to the magnetopause. Using observations from Voyagers 1 and 2, Cattaneo et al. (1998) found that mirror structures could evolve from quasi-sinusoidal to nonperiodic structures from

a quasi-perpendicular bow shock to a low-shear magnetopause. During propagation, the wave may evolve to different types of MMWs and sometimes convert to an EMIC structure. We also noticed that the frequency of an MMW shifted slightly to a lower value from the bow shock to the magnetopause, which may be associated with energy dissipation. Mirror mode waves play a role in regulating particle distribution and energy dissipation in the magnetosheath. Free energy associated with the magnetic field and plasma distributions are different in different regions of the planetary magnetosheath, such as near the bow shock, the middle magnetosheath, and the magnetopause. This may lead to MMW excitation of a different magnetic morphology and frequency, which also reflects different energy dissipation processes. For example, the interaction between MMWs and the magnetopause may lead to periodic energy dissipations in the magnetopause. This finding requires further statistical investigation of their features and physical mechanisms. The mechanisms for wave evolution also need further investigation. In addition, a statistical study of the wave distribution to local time and the radial distance could significantly aid in global understanding of the MMWs in Saturn's magnetosheath. Because the solar wind is an important condition for generating MMWs near the bow shock, the connection between the solar wind condition and the features of MMWs also needs investigation.

Acknowledgments

References

Achilleos, N., Bertucci, C., Russell, C. T., Hospodarsky, G. B., Rymer, A. M., Arridge, C. S., Burton, M. E., Dougherty, M. K., Hendricks, S., … Tsurutani, B. T. (2006). Orientation, location, and velocity of Saturn's bow shock: initial results from the Cassini spacecraft. *J. Geophys. Res.: Space Phys.*, *111*(A3), A03201. https://doi.org/10.1029/2005JA011297

Cattaneo, M. B. B., Basile, C., Moreno, G., and Richardson, J. D. (1998). Evolution of mirror structures in the magnetosheath of Saturn from the bow shock to the magnetopause. *J. Geophys. Res.: Space Phys.*, *103*(A6), 11961–11972. https://doi.org/10.1029/97JA03683

Génot, V., Schwartz, S. J., Mazelle, C., Balikhin, M., Dunlop, M., and Bauer, T. M. (2001). Kinetic study of the mirror mode. *J. Geophys. Res.: Space Phys.*, *106*(A10), 21611–21622. https://doi.org/10.1029/2000JA000457

Génot, V., Budnik, E., Hellinger, P., Passot, T., Belmont, G., Trávníček, P. M., Sulem, P. L., Lucek, E., and Dandouras, I. (2009). Mirror structures above and below the linear instability threshold: cluster observations, fluid model and hybrid simulations. *Ann. Geophys.*, *27*(2), 601–615. https://doi.org/10.5194/angeo-27-601-2009

Glassmeier, K. H., Motschmann, U., Mazelle, C., Neubauer, F. M., Sauer, K., Fuselier, S. A., and Acuña, M. H. (1993). Mirror modes and fast magnetoacoustic waves near the magnetic pileup boundary of comet P/Halley. *J. Geophys. Res.: Space Phys.*, *98*(A12), 20955–20964. https://doi.org/10.1029/93ja02582

Hasegawa, A. (1969). Drift mirror instability in the magnetosphere. *Phys. Fluids*, *12*(12), 2642. https://doi.org/10.1063/1.1692407

Joy, S. P., Kivelson, M. G., Walker, R. J., Khurana, K. K., Russell, C. T., and Paterson W. R. (2006). Mirror mode structures in the Jovian magnetosheath. *J. Geophys. Res.: Space Phys.*, *111*, A12212. https://doi.org/10.1029/2006JA011985

Kaufmann, R. L., Horng, J. T., and Wolfe, A. (1970). Large-amplitude hydromagnetic waves in the inner magnetosheath. *J. Geophys. Res.: Space Phys.*, *75*(25), 4666–4676. https://doi.org/10.1029/JA075i025p04666

Lucek, E. A., Dunlop, M. W., Balogh, A., Cargill, P., Baumjohann, W., Georgescu, E., Haerendel, G., and Fornacon, G. H. (1999). Identification of magnetosheath mirror modes in Equator-S magnetic field data. *Ann. Geophys.*, *17*(12), 1560–1573. https://doi.org/10.1007/s00585-999-1560-9

Mazelle, C., Belmont, G., Glassmeier, K. H., Le Quéau, D., and Rème, H. (1991). Ultra low frequency waves at the magnetic pile-up boundary of comet P/Halley. *Adv. Space Res.*, *11*(9), 73–77. https://doi.org/10.1016/0273-1177(91)90014-b

Price, C. P., Swift, D. W., and Lee, L. C. (1986). Numerical simulation of nonoscillatory mirror waves at the Earth's magnetosheath. *J. Geophys. Res.: Space Phys.*, *91*(A1), 101–112. https://doi.org/10.1029/JA091iA01p00101

Russell, C. T., Riedler, W., Schwingenschuh, K., and Yeroshenko, Y. (1987). Mirror instability in the magnetosphere of comet Halley. *Geophys. Res. Lett.*, *14*(6), 644–647. https://doi.org/10.1029/GL014i006p00644

Russell, C. T., Kivelson, M. G., Khurana, K. K., and Huddleston, D. E. (1998). Magnetic fluctuations close to Io: ion cyclotron and mirror mode wave properties. *Planet. Space Sci.*, *47*(1–2), 143–150. https://doi.org/10.1016/S0032-0633(98)00090-7

Russell, C. T., Leisner, J. S., Arridge, C. S., Dougherty, M. K., and Blanco-Cano, X. (2006). Nature of magnetic fluctuations in Saturn's middle magnetosphere. *J. Geophys. Res.: Space Phys.*, *111*(A12), A12205. https://doi.org/10.1029/2006JA011921

Shoji, M., Omura, Y., Tsurutani, B. T., Verkhoglyadova, O. P., and Lembege, B. (2009). Mirror instability and L-mode electromagnetic ion cyclotron instability: competition in the Earth's magnetosheath. *J. Geophys. Res.: Space Phys.*, *114*(A10), A10203. https://doi.org/10.1029/2008JA014038

Soucek, J., Escoubet, C. P., and Grison, B. (2015). Magnetosheath plasma stability and ULF wave occurrence as a function of location in the magnetosheath and upstream bow shock parameters. *J. Geophys. Res.: Space Phys.*, *120*(4), 2838–2850. https://doi.org/10.1002/2015JA021087

Sulaiman, A. H., Masters, A., Dougherty, M. K., Burgess, D., Fujimoto, M., and Hospodarsky, G. B. (2015). Quasiperpendicular high mach number shocks. *Phys. Rev. Lett.*, *115*(12), 125001. https://doi.org/10.1103/PhysRevLett.115.125001

Sulaiman, A. H., Masters, A., and Dougherty, M. K. (2016). Characterization of Saturn's bow shock: magnetic field observations of quasi-perpendicular shocks. *J. Geophys. Res.: Space Phys.*, *121*(5), 4425–4434. https://doi.org/10.1002/2016JA022449

Tátrallyay, M., and Erdős, G. (2005). Statistical investigation of mirror type magnetic field depressions observed by ISEE-1. *Planet. Space Sci.*, *53*(1–3), 33–40. https://doi.org/10.1016/j.pss.2004.09.026

Thomsen, M. F., Coates, A. J., Jackman, C. M., Sergis, N., Jia, X., and Hansen, K. C. (2018). Survey of magnetosheath plasma properties at Saturn and inference of upstream flow conditions. *J. Geophys. Res.: Space Phys.*, *123*(3), 2034–2053. https://doi.org/10.1002/2018JA025214

Tsurutani, B. T., Smith, E. J., Anderson, R. R., Ogilvie, K. W., Scudder, J. D., Baker, D. N., and Bame, S. J. (1982). Lion roars and nonoscillatory drift mirror waves in the magnetosheath. *J. Geophys. Res.: Space Phys.*, *87*(A8), 6060. https://doi.org/10.1029/JA087iA08p06060

Tsurutani, B. T., Lakhina, G. S., Verkhoglyadova, O. P., Echer, E., Guarnieri, F. L., Narita, Y., and Constantinescu, D. O. (2011). Magnetosheath and heliosheath mirror mode structures, interplanetary magnetic decreases, and linear magnetic decreases: differences and distinguishing features. *J. Geophys. Res.: Space Phys.*, *116*(A2), A02103. https://doi.org/10.1029/2010JA015913

Violante, L., Cattaneo, M. B. B., Moreno, G., and Richardson, J. D. (1995). Observations of mirror waves and plasma depletion layer upstream of Saturn's magnetopause. *J. Geophys. Res.: Space Phys.*, *100*(A7), 12047–12055. https://doi.org/10.1029/94JA02703

Volwerk, M., Zhang, T. L., Delva, M., Vörös, Z., Baumjohann, W., and Glassmeier, K. H. (2008a). Mirror-mode-like structures in Venus' induced magnetosphere. *J. Geophys. Res.: Planets*, *113*(E9), E00B16. https://doi.org/10.1029/2008je003154

Volwerk, M., Zhang, T. L., Delva, M., Vörös, Z., Baumjohann, W., and Glassmeier, K. H. (2008b). First identification of mirror mode waves in Venus' magnetosheath?. *Geophys. Res. Lett.*, *35*(12), L12204. https://doi.org/10.1029/2008gl033621

Volwerk, M., Glassmeier, K. H., Delva, M., Schmid, D., Koenders, C., Richter, I., and Szegö, K. (2014). A comparison between VEGA 1, 2 and Giotto flybys of comet 1P/Halley: implications for Rosetta. *Ann. Geophys.*, *32*(11), 1441–1453. https://doi.org/10.5194/angeo-32-1441-2014

Volwerk, M., Richter, I., Tsurutani, B., Götz, C., Altwegg, K., Broiles, T., Burch, J., Carr, C., Cupido, E. … Glassmeier, K. H. (2016). Mass-loading, pile-up, and mirror-mode waves at comet 67P/Churyumov-Gerasimenko. *Ann. Geophys.*, *34*(1), 1–15. https://doi.org/10.5194/angeo-34-1-2016

Winterhalter, D., Neugebauer, M., Goldstein, B. E., Smith, E. J., Tsurutani, B. T., Bame, S. J., and Balogh, A. (1995). Magnetic holes in the solar wind and their relation to mirror-mode structures. *Space Sci. Rev.*, *72*, 201–204. https://doi.org/10.1007/BF00768780

Zhang, T. L., Baumjohann, W., Russell, C. T., Jian, L. K., Wang, C., Cao, J. B., Balikhin, M., Blanco-Cano, X., Delva, M., and Volwerk, M. (2009). Mirror mode structures in the solar wind at 0.72 AU. *J. Geophys. Res.: Space Phys.*, *114*(A10), A10107. https://doi.org/10.1029/2009JA014103